Dynamics of atomic species involved in shear-induced displacements at sliding symmetrical grain boundaries: a numerical study

2007 J. Phys.: Condens. Matter 19 096008

(http://iopscience.iop.org/0953-8984/19/9/096008)

IOP PUBLISHING JOURNAL OF PHYSICS: CONDENSED MATTER

J. Phys.: Condens. Matter **19** (2007) 096008 (14pp) doi:10.1088/0953-8984/19/9/096008

Dynamics of atomic species involved in shear-induced displacements at sliding symmetrical grain boundaries: a numerical study

Francesco Delogu

Dipartimento di Ingegneria Chimica e Materiali, Università degli Studi di Cagliari, piazza d'Armi, I-09123 Cagliari, Italy

E-mail: delogu@dicm.unica.it

Received 2 November 2006, in final form 19 January 2007
Published 12 February 2007
Online at stacks.iop.org/JPhysCM/19/096008

Abstract

Molecular dynamics methods have been used to study the mechanical response under shear of two Cu systems containing symmetrical tilt and twist grain boundaries, respectively. The investigation focuses on the mechanism of localized atomic displacements during plastic deformation. It is shown that grain boundary sliding generates a perturbed layer of atomic species, with thickness increasing approximately with the square root of time. The dynamics of the atomic displacement processes, even though apparently stochastic, is intimately connected with the local density experienced by atoms under shear.

(Some figures in this article are in colour only in the electronic version)

1. Introduction

Severe plastic deformation of solid phases can induce anomalous mass transport phenomena over a wide range of length scales [1–3]. Such phenomena underlie the mechanical methods of powder metallurgy, where elemental metals progressively interpenetrate as a consequence of the enhanced atomic mobility due to elementary distortion events [4–6]. The gradual refinement of the microstructure down to the nanometre range is accompanied by a fine mixing of chemical species, often resulting in the formation of metastable alloys [6]. This apparently simple picture hides a complex mix of intertwined processes that are still challenging to modern science, the atomic-scale mechanisms being a matter of lively debate [7]. The initially invoked thermal diffusion scenarios have been undermined by approaches that lay emphasis on the forced mixing of chemical elements under extensive plastic straining, the fine details of which have been explored by numerical simulations [8–16]. These have shown that the accumulation of lattice defects and disorder can induce the amorphization of a crystalline structure even in the absence of thermal effects [12, 13]. Depending on temperature, the dynamical competition between mechanically forced mixing and thermally

activated decomposition governs the formation of compositional patterns in immiscible alloy systems [8, 9, 16]. However, mechanical effects can here also result in chemical ordering at low temperature, originating from the dependence of forced mixing on the length scale [16]. Forced mixing was also shown to occur at sheared interfaces, the thickness of the intermixed layer scaling with the square root of time [11, 14, 15]. An unexpected parallel between forced mixing and thermal diffusion has thus arisen, suggesting a stochastic mechanism for shear-induced atomic migration.

The present work attempts to gain further insight along such lines of enquiry by employing molecular dynamics simulations to study the atomic displacement processes taking place at sliding interfaces. The atomic dynamics under shear has been explored for two different interfaces, namely the $\Sigma 11$ (332) symmetrical tilt and $\Sigma 29$ (001) symmetrical twist grain boundaries. The two systems have recently been subjected to detailed studies concerning grain boundary structure, energy and mobility [17, 18]. Their use in this work then represents a unique opportunity to test the reliability of the numerical methods employed and throw light on the microscopic mechanical response of a grain boundary under simple shear.

2. Molecular dynamics simulations

Calculations were carried out on so-called bi-crystals of Cu atoms in the face-centred cubic (fcc) lattice with $cF4$ structure containing different interfaces. In the first case, a configuration of 38 737 atoms was used. Atoms were arranged in two semi-crystals with face-centred-cubic (fcc) $cF4$ structure constructed according to the coincident site lattice (CSL) model [17, 19]. The grain boundary (GB) plane is parallel to the $(x; y)$ plane, and the semi-crystals were tilted around the $\langle 110 \rangle$ vector by 50.48°. Each semi-crystal was generated by repeating the CSL cell along the three Cartesian directions. The relaxed simulation cell has dimensions of about 8, 7 and 8.5 nm, respectively, along the x, y and z Cartesian directions.

In the second case, 31 900 atoms were arranged in two semi-crystals with fcc $cF4$ structure consisting of a stacking sequence of 22 (001) atomic planes separated by a so-called $\Sigma 29$ (001) symmetrical twist boundary. The grain boundary was obtained by rotating one semi-crystal relative to the other by an angle of 43.6° about the (001) plane normal along the z Cartesian direction, the $(x; y)$ plane being parallel to the GB [20]. The dimensions of the relaxed simulation cell are about 7 nm along the x and y Cartesian directions and 8 nm along the z direction. Snapshots of the GBs are shown in figure 1 for the sake of illustration.

Periodic boundary conditions (PBCs) were imposed along the x and y Cartesian directions, whereas along the z Cartesian direction the simulation cell terminates with two reservoir regions containing both immobile and mobile species [10, 20]. Each reservoir has a thickness of about 1.5 nm and immobile atoms are confined to the most external layer, which is 0.8 nm thick—a value determined by the cutoff radius of the interatomic potential [10, 20]. The latter was described by a semi-empirical many-body tight-binding force scheme based on the second-moment approximation to the electronic density of states [21–23]. Interactions were computed within a spherical cutoff radius of about 0.7 nm, which allows for a satisfactory reproduction of thermodynamic and elastic properties [23]. The potential parameter values were taken from the literature [23]. The equations of motion were solved by employing a fifth-order predictor–corrector algorithm [24] with a time step of 2.0 fs.

The systems were equilibrated in the isobaric-isothermal *NPT* ensemble at 300 K and null external pressure. In the first case, equilibration was carried out for 200 ps. In the second case, semi-crystals were separately relaxed for 30 ps and then approached along the z Cartesian direction up to the distance of minimum enthalpy [20]. The resulting configuration was further equilibrated for 20 ps. In both cases, during the relaxation stages the Nosè–Hoover thermostat

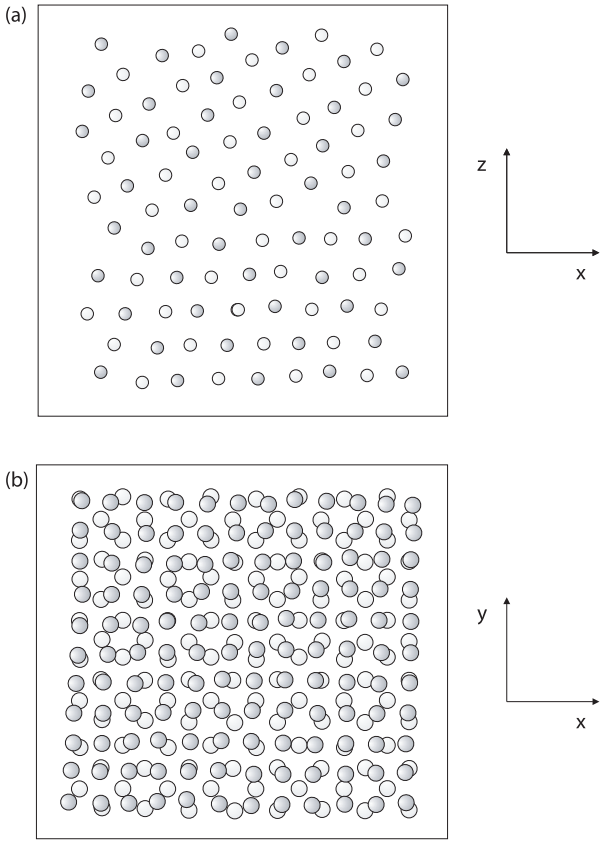

Figure 1. The geometries of the Σ11 (332) ⟨110⟩ symmetrical tilt GB (a) and the Σ29 (001) symmetrical twist GB (b). Configurations of minimum potential energy are shown. Only two interfacial atomic planes are shown for the sake of clarity. Light and dark grey atoms belong respectively to lower and upper planes.

and the Parrinello–Rahman scheme were implemented over all the mobile atoms [25–27]. After the application of tangential forces, the thermostat was applied only to mobile reservoir atoms to avoid stochastic coupling with a thermal bath and permit a spontaneous distribution of kinetic energy under shear.

A normal force F_n along the z Cartesian direction was applied to reservoir atoms at the end of the relaxation stages to produce a small uniaxial stress of about 0.1 MPa. A roughly constant distance between the reservoirs was therefore kept and local strains were efficiently accommodated [10, 14, 15]. A tangential force F_t was applied to reservoirs along the x Cartesian direction to simulate the effects of a shear stress [10, 14, 15]. Centre-of-mass velocities $+u_p/2$ and $-u_p/2$ were correspondingly given to the upper and lower reservoirs, respectively. A relative sliding velocity, u_p, of 10 m s^{-1}, close to the minimum threshold to induce shear deformation in times accessible to computer simulations, was used to keep the strain rate as low as possible [10, 14, 15, 28]. A velocity field with a linear profile in the range between $-u_p/2$ and $+u_p/2$ was also imposed for 2 ps to the atoms outside the reservoirs to favour the attainment of homogeneous shear behaviour and to avoid shock waves [14, 15, 28]. Characteristic features of the simulation cell and the forces applied are depicted schematically in figure 2(a).

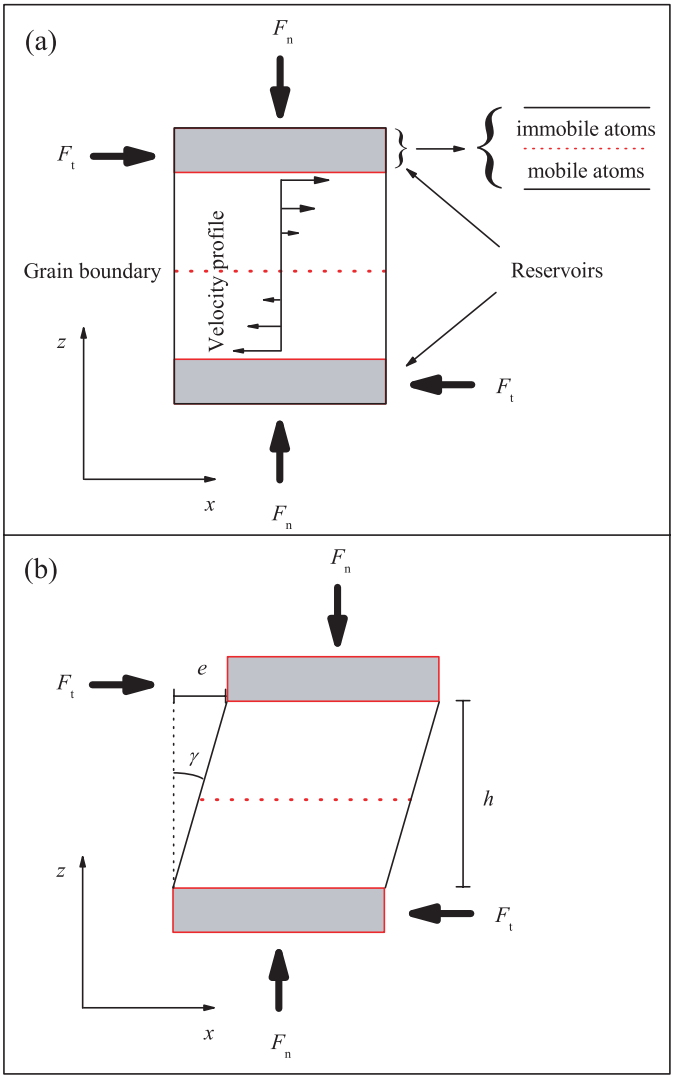

Figure 2. (a) A schematic illustration of the simulation cell. The structure of the reservoir regions is shown explicitly. The velocity profile, symmetrical with respect to the GB position at the centre of the cell, is also quoted. (b) Geometry of deformation under the action of normal and tangential forces, F_n and F_t.

Once normal and tangential forces are applied, the simulation cell undergoes a mechanical deformation, as shown in figure 2(b). The shear strain γ is thus given by the relationship

$$\gamma = \arctan\left(\frac{e}{h}\right), \tag{1}$$

where e corresponds to the shear displacement and h to the distance between reservoirs. The local stress tensor β^i_{km} was evaluated for each atom i according to the expression [28]

$$\beta^i_{km} = \frac{1}{\Omega^i}\sum_{j\neq i}^{N_{nn}} f^{ij}_k r^{ij}_m, \tag{2}$$

where Ω^i is the atomic volume, $\boldsymbol{f}_k^{ij}$ and $\boldsymbol{r}_m^{ij}$ are respectively the force and the position vectors connecting the atoms i and j, and N_{nn} is the number of nearest neighbours of atom i. The stress tensor σ_{km} was then defined as [28]

$$\sigma_{km} = \frac{1}{N^*} \sum_{i}^{N^*} \beta_{km}^i, \tag{3}$$

with N^* representing the number of mobile non-reservoir atoms. This average stress, hereafter indicated by σ, was used to evaluate the stress–strain response of the system as well as its yield point. The atomic volume Ω^i was estimated *via* the well-known Voronoi space tessellation [29, 30]. More specifically, Voronoi polyhedra were defined around each atom and their volumes evaluated according to standard numerical methods.

It is worth noting here that the relatively small size of the simulation cell and the high strain rates correspondingly obtained, on the order of 1×10^7 s^{-1}, do not allow any reliable comparison with experimental findings. Usual experiments of shear deformation indeed employ strain rates of about 10^3–10^4 s^{-1}, which is roughly three to four orders of magnitudes lower. Strain rates on the order of 10^7–10^8 s^{-1} can exceptionally be attained under experimental conditions only when nanometre-sized particles are deformed at high rates. In any case, the results obtained in the present work should be regarded as only indicative.

It should also be noted that the existence of reservoir regions can have important consequences on the mechanical behaviour of crystalline systems under deformation. Immobile atomic species indeed induce an anomalous ordering in the adjacent atomic planes, thus affecting the dynamics of atomic species located there. Such an effect is however relatively short-ranged and disappears at distances of about 0.4 nm. In principle, the presence of immobile species can also modify the dynamical behaviour of atoms, up to the point of affecting the processes of dislocation nucleation and motion, which of course underlie the whole mechanical deformation. In the present case, such shortcomings are in part avoided as a consequence of the inclusion of mobile species in the reservoir region.

The degree of structural order, as well as the eventual shear-induced migration of the GBs, were monitored by means of the static order parameter [24],

$$S(\boldsymbol{k}) = \frac{1}{N} \left\{ \left[\sum_{i=1}^{N} \cos(\boldsymbol{k} \cdot \boldsymbol{r}^i) \right]^2 + \left[\sum_{i=1}^{N} \sin(\boldsymbol{k} \cdot \boldsymbol{r}^i) \right]^2 \right\}^{\frac{1}{2}}, \tag{4}$$

where the wavevector $\boldsymbol{k}$ is a reciprocal lattice plane vector and $\boldsymbol{r}^i$ is the vector defining the position of the ith atom. N is the total number of mobile atoms. For each bi-crystal, the region of mobile atoms between the two reservoirs was divided into 16 slices, each roughly 4.2 Å thick. Given that computations were performed in the *NPT* ensemble, with a consequent variation of the simulation cell volume, the slice thickness was re-calculated at each step.

Local structural order was quantified through analysis of the coordination shell according to the Honeycutt–Andersen methodology [31]. In addition, the so-called centrosymmetry parameter, P, was employed in accordance with the following definition [32]:

$$P = \sum_{i=1}^{6} |\boldsymbol{R}_i + \boldsymbol{R}_{i+6}|^2. \tag{5}$$

Here, $\boldsymbol{R}_i$ and $\boldsymbol{R}_{i+6}$ represent the vectors connecting the six pairs of nearest neighbours surrounding a given atom in a relaxed fcc lattice. According to the original analysis [32], Cu atoms involved in perfect fcc lattice sites, in partial dislocations, in stacking faults and in surfaces, exhibit P values roughly equal to 0, 1.65, 6.51 and 19.5 Å^2 respectively. As suggested

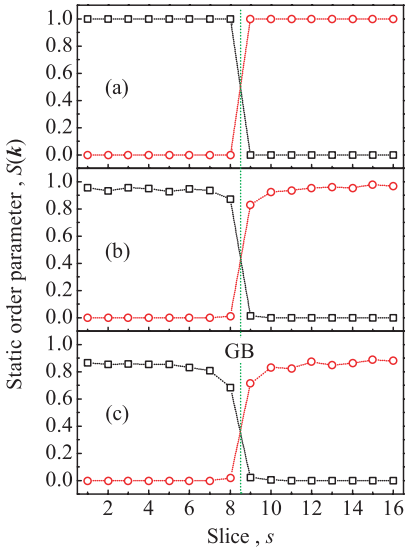

Figure 3. The static order parameter $S(\boldsymbol{k})$ values for the different slices s in which the bi-crystal region between reservoirs is divided. Data refer to (a) the initial configuration, (b) the thermally equilibrated configuration, and (c) the configuration attained after 0.5 ns under shear in the system containing the $\Sigma 29$ (001) symmetrical twist GB. The vertical dotted line marks the GB position.

in the literature [32], it is however preferable to use the range of values to distinguish between different topologies of defects. Atoms involved in partial dislocations were thus defined as those with P values in the range between 0.39 and 3.14 Å^2. A further check was carried out in this case by analysing the well-known topological constraints on the circuits of the Burgers' vector. Stacking faults and surfaces were instead regarded as containing atoms with P values in the range between 3.14 and 15.20 Å^2 and larger than 15.20 Å^2, respectively.

3. Results and discussion

The $\Sigma 11$ (332) ⟨110⟩ symmetrical tilt and the $\Sigma 29$ (001) symmetrical twist GBs have been shown to be relatively mobile GBs with a significant tendency to migrate, with different mechanisms, in the normal direction [17–20, 33]. Either mechanical forces or thermal driving forces must, however, be present in the system. The former condition is met when an anisotropic elastic stress is imposed to the simulation cell, whereas the latter requires relatively high temperatures. It is worth noting here that none of these conditions is satisfied in the present calculations, given the symmetrical application of mechanical forces and the low temperature at which computations are carried out. As a consequence, no significant migration of the GBs along the z Cartesian direction is expected. Numerical findings proved that such expectations were founded, as shown by the data quoted in figure 3 where the $S(\boldsymbol{k})$ values for the different slices in which the bi-crystals were divided are reported at different times. Figure 3 refers to the $\Sigma 29$ (001) symmetrical twist GB, but similar results are found in the other case. It can be seen that the GB does not undergo significant positional changes, remaining roughly at the centre of the simulation box. Once the shear forces are applied, the fluctuations around the average position increase as a consequence of the GB atomic dynamics underlying the mechanical behaviour of the bi-crystal under shear.

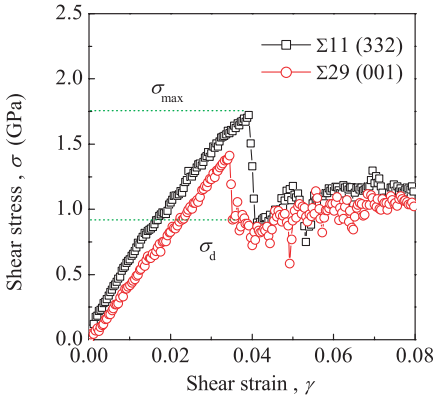

Figure 4. The mechanical response under shear of the two bi-crystals considered. The onset of plastic deformation at the Σ29 (001) symmetrical twist GB occurs at shear stress σ and shear strain γ values slightly smaller than for the Σ11 (332) ⟨110⟩ symmetrical tilt GB.

The mechanical response of the bi-crystals under shear is illustrated in figure 4, where the average stress σ is quoted as a function of the average strain γ. The two bi-crystals exhibit similar trends, although significant quantitative differences are observed. The curves point out the existence of two different deformation regimes. The initial increase in the average stress σ with the average strain γ is roughly linear, due to the approximate proportionality with the modulus of rigidity G of the two quantities when deformation is elastic. After reaching a maximum stress value $\sigma_{\max}$ at the average strain $\gamma_{\max}$, a sudden drop to a lower value, σ_d, is observed. Such a drop marks the occurrence of a transition between the elastic regime to the plastic deformation regime and then the onset of sliding behaviour at the GB. The abrupt stress relaxation is associated with the nucleation of dislocations. Further increases in the average strain γ give rise to a continuous irregular change in the average stress that is reminiscent of so-called stick-and-slip processes [17]. Both systems tend to reach the same approximate plateau value of average stress σ.

The bi-crystal containing the Σ29 (001) symmetrical twist GB undergoes elastic-to-plastic deformation transition at a shear strain $\gamma_{\max}$ roughly amounting to 0.034. The $\gamma_{\max}$ value for the system containing the Σ11 (332) ⟨110⟩ symmetric tilt GB amounts instead to about 0.039, in excellent agreement with previous estimates [17]. In this latter case, a satisfactory agreement with literature values [17] is also obtained for the $\sigma_{\max}$ and σ_d quantities, roughly equal to 1.74 and 0.85 GPa respectively. In the case of the bi-crystal with the twist GB, the $\sigma_{\max}$ and σ_d values amount to about 1.41 and 0.92 GPa, respectively. Such values should be compared with those pertaining to a perfect, surface-free Cu crystal, amounting respectively to about 4.3 and 1.9 GPa, obtained by ad hoc simulations carried out on a Cu crystal of 32 000 atoms and in accordance with literature estimates under similar simulation conditions [28]. Although the two systems that were investigated display similar behaviour, it appears that the Σ29 (001) symmetrical twist GB undergoes plastic deformation under conditions less severe than for the Σ11 (332) ⟨110⟩ symmetric tilt GB. The same result was obtained in six independent simulations carried out under different initial conditions in order to test the reliability of the dynamics observed. This result could tentatively be related to the average GB energy, evaluated as the difference between the total energies of the bi-crystals and of a perfect bulk system [17]. The largest GB energy, roughly amounting to 0.742 J m^{-2} in satisfactory agreement with previous work [20], was indeed found to pertain to the bi-crystal containing the Σ29 (001)

symmetrical twist GB. Such a value is about 10% larger than the GB energy of the $\Sigma 11$ (332) $\langle 110 \rangle$ symmetric tilt GB, approximately equal to 0.681 J m^{-2}. Also this estimate compares well with the one reported in previous work [17]. The results mentioned above suggest that the GB with the largest content of energy, i.e. the less stable one, is the GB that most easily undergoes the elastic-to-plastic deformation transition. However, previous research work [17, 33] has clearly pointed out that the onset and the mechanistic features of the sliding behaviour are not simply correlated to the GB energy. On the contrary, they rather depend on the structural units characterizing the GB atomic arrangement. On such a basis, the possible connection between the GB energy and the onset of sliding processes inferred in this work should be considered with great attention, and by no means should be intended as conclusive.

As briefly mentioned above, after the $\sigma_{\max}$ value has been attained and the abrupt decrease to σ_d has occurred, deformation takes place under plastic conditions. Correspondingly, partial dislocations nucleate at the GBs as a consequence of localized shear events favoured by a decrease in the average atomic density at the sliding interface. Sliding is preceded by so-called shuffling processes restricted to a small number of atomic species at GBs. These atoms gradually undergo a separation of their dynamical regime from that of the reminder of the bi-crystal, showing a decreasing correlation of their displacements with those performed by their neighbours. Such behaviour is strongly associated with a decrease in the local density at the interface. A few atoms involved in shuffling events or some of their nearest neighbours indeed possess atomic volumes Ω about 10% larger than the volume Ω_{bulk} of unperturbed bulk atoms. This can be inferred clearly from figures 5(a) and (b), which focus on the same GB region. Figure 5(a) shows the GB atoms with volume Ω larger than $1.08\Omega_{\text{bulk}}$, whereas figure 5(b) shows the GB atoms involved in shuffling processes in the succeeding 1 ps.

The GB regions in which atomic shuffling processes take place as a consequence of a density decrease are also involved in the nucleation and eventual propagation of partial dislocations in the semi-crystals. This can be seen from figure 6, where the GB region depicted in detail in figure 5 is shown about 200 ps later.

The GB sliding and the correlated atomic shuffling processes determine the occurrence of a pronounced roughening of the initially smooth GB interface. Correspondingly, the coordination shells of single atoms undergo increasing distortions, immediately pointed out by a general increase in the centrosymmetry parameter P. The rise in P values is particularly evident for interfacial atoms that are already involved in the GB structure. Within a relatively short time from the onset of sliding behaviour, the redistribution of excess free volume resulting from the atomic shuffling underlying the nucleation and propagation of partial dislocations induces an anomalous mobility of GB atoms. These repeatedly become involved in displacement processes that gradually promote the exchange of atoms between opposite sides of the GB. More specifically, atoms belonging to one of the semi-crystals at a given time are found to belong to the other semi-crystal at a succeeding time. In addition, the whole GB region evolves with time under sliding conditions. This is shown clearly by the fact that single atoms are seen to migrate from the GB interface to the interior of the semi-crystals and vice versa. In other words, a shear-induced mixing process takes place, progressively involving a larger number of atoms at or close to the original interface. The mixing of atoms belonging to the two semi-crystals was monitored quantitatively by means of the parameter [11]

$$\delta(z,t) = \frac{1}{n}\left\{\sum_{i=1}^{n}|z_i(t) - z_i(0)| - \left|\sum_{i=1}^{n}[z_i(t) - z_i(0)]\right|\right\}, \tag{6}$$

where $z_i(t)$ and $z_i(0)$ are respectively the z Cartesian coordinates of the ith atom at times t and 0. n is the number of atoms with initial coordinates between z and $z + \mathrm{d}z$. The first term

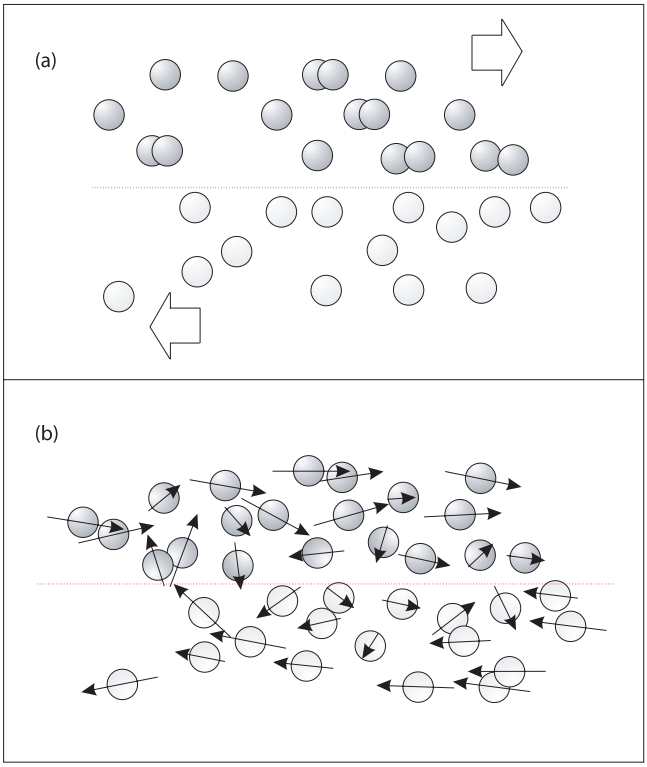

Figure 5. (a) A snapshot of the species with atomic volume Ω larger than 1.08 Ω_{bulk} at the Σ29 (001) symmetrical twist GB. (b) Atoms involved in shuffling processes in the same region after a time delay of 1 ps. Small arrows indicate the direction and modulus of velocity. Large arrows indicate the direction of application of shear forces. The horizontal dotted lines roughly mark the position of the GB. For the sake of clarity, only the positions of atoms in a vertical region 0.3 nm thick are projected on the $(x; z)$ plane. Light and dark grey indicate atoms located on different sides of the GB.

represents the total amount of displacement along the z Cartesian direction within a layer of thickness dz, whereas the second term measures the fraction of displacement due to the possible shift in the centre of mass of such a layer [11]. The larger the $\delta(z, t)$ value, the further the atoms move from their original positions, determining a higher degree of mixing.

As shown in figure 7(a), $\delta(z, t)$ can be fitted satisfactorily with a Gaussian function centred at z_0, which at all times roughly corresponds to the position along the z Cartesian direction of the original GB interface. The rough constancy of the z_0 value, apart from providing additional evidence of the absence of significant GB migration processes, indicates that mass transport phenomena take place with greater efficiency at the GB interface. The height of $\delta(z, t)$ at the GB interface, i.e. $\delta(z_0, t)$, provides a measure of the thickness of the mixed layer [11], and its dependence on time t is shown in figure 7(b). It can be seen that $\delta(z_0, t)^2$ scales with t according to a roughly linear trend for both systems under scrutiny. Such scaling reveals that the mixed layer thickness grows with kinetics analogous to the those observed in case of thermal diffusion [11]. Analogous scaling is obtained when a different measure of the mixed layer thickness is adopted, e.g. when it is estimated by the difference between the z Cartesian coordinates of the Cu atoms characterized by the largest penetration distances into the semi-crystal to which they originally do not belong.

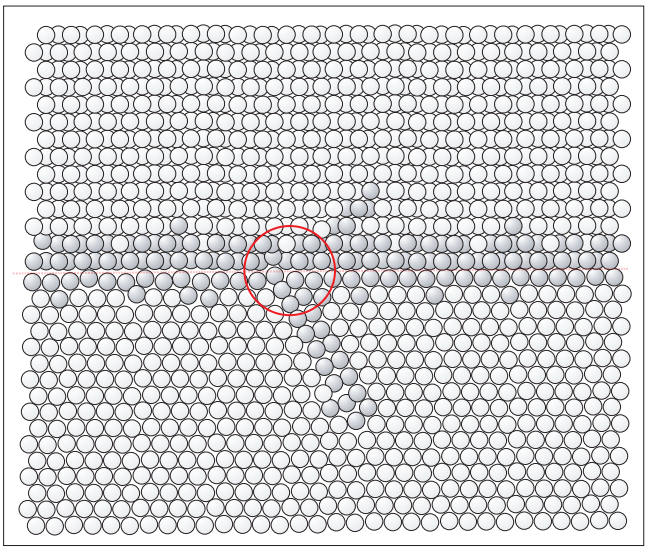

Figure 6. A snapshot of the Σ29 (001) symmetrical twist GB about 200 ps later than the configurations shown in figure 5. Dark grey indicates atoms with a centrosymmetry parameter P larger than 0.3. A partial dislocation can be observed in the lower semi-crystal. The horizontal dotted line roughly marks the GB position. The circle identifies the GB region shown in detail in figure 5 at which the partial dislocations has nucleated. Only atoms within a layer about 0.3 nm thick are shown for the sake of clarity.

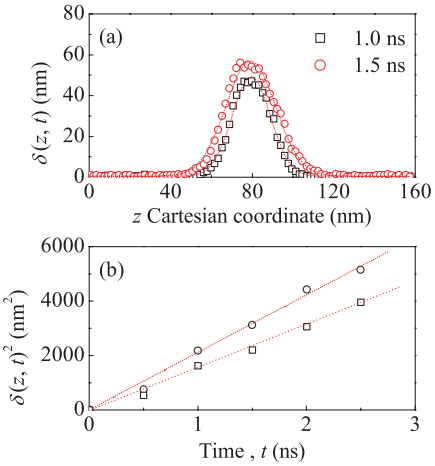

Figure 7. (a) The mixing parameter $\delta(z, t)$ as a function of the z Cartesian coordinate at the times quoted. Data refer to the system containing the Σ29 (001) symmetrical twist GB. (b) The linear scaling of $\delta(z_0, t)^2$ with time t for the systems containing Σ11 (332) ⟨110⟩ symmetrical tilt (□) and the Σ29 (001) symmetrical twist (○) GBs. The best-fitted Gaussian curves and lines are shown.

The mechanism underlying the atomic displacement and mixing processes is, however, deeply different from the one characteristic of thermal diffusion. Depending on the free volume locally available, atoms move according to cooperative processes involving the contemporary displacement of various atoms. This can be seen by directly visualizing the atomic configurations at different times, as well as by analysing their relative dynamics in

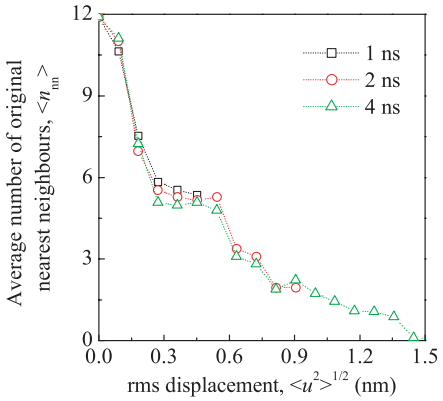

Figure 8. The dependence of the number of original nearest neighbours $\langle n_{nn} \rangle$ on the rms displacement $\langle u^2 \rangle^{1/2}$ at the times quoted. The curves have a similar shape, displaying step-like decreases at distances roughly corresponding to integer and semi-integer multiples of either the (001) or the (111) plane spacing. Data refer to the system containing the $\Sigma 29$ (001) symmetrical twist GB.

detail, which permits the identification of strings of atoms with correlated motion [33]. In order to gain additional information, cooperative displacements were here characterized by monitoring the coordination shells of displacing atoms. To this aim, the nearest neighbours of each given atom were identified at the beginning of the simulation and their gradual replacement related to the root-mean-square (rms) displacement, $\langle u^2 \rangle^{1/2}$, of the atom [24]. The number and identity of nearest neighbours were ascertained at each time step by applying a distance criterion according to which nearest neighbours are located at distances r smaller than the 1, r_{min}, at which the pair correlation function has its first minimum [34]. The atoms were classified according to their $\langle u^2 \rangle^{1/2}$, and the average number $\langle n_{nn} \rangle$ of original nearest neighbours was estimated by averaging n_{nn} over the atoms with rms displacement $\langle u^2 \rangle^{1/2}$ within a given small interval. The curves obtained at three different times are reported in figure 8 for the bi-crystal containing the $\Sigma 29$ (001) symmetrical twist GB. Similar results were found for the other system investigated. As expected, $\langle n_{nn} \rangle$ decreases as $\langle u^2 \rangle^{1/2}$ increases. The curves obtained at different times display considerable superposition, thus suggesting that the replacement of atoms belonging to the original coordination shells is strongly correlated to the distance travelled by atoms. Furthermore, the step-like decrease in the average number, $\langle n_{nn} \rangle$, of original nearest neighbours points out the existence of most probable distances at which a displacing atom loses its neighbours. In the case of the bi-crystal containing the $\Sigma 29$ (001) symmetrical twist GB, such distances roughly correspond to integer and semi-integer multiples of either the (001) or the (111) plane spacings. The bi-crystal containing the $\Sigma 11$ (332) $\langle 110 \rangle$ symmetrical tilt GB gives rise to an analogous behaviour, although the distance at which the first drop in $\langle n_{nn} \rangle$ cannot be related to the spacing between planes with low Miller indices. The data in figure 8 show that about three original nearest neighbours are still retained by atoms that travelled distances on the order of 0.7 nm. According to the above-mentioned numerical findings, atoms do not undergo isolated displacements in which the role of nearest neighbours is restricted to so-called 'cage effects', as in the case of thermal diffusion. In contrast, atoms experience a series of cooperative rearrangements during which a fraction of nearest neighbours follows the displacing atom.

Once the regime of plastic deformation has been attained, a significant fraction of atoms approximately located in the GB region of lower density follows trajectories closely resembling

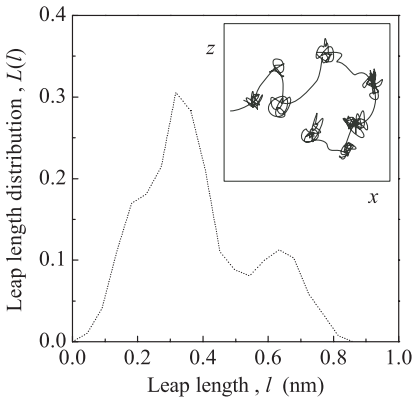

Figure 9. The distribution $L(l)$ of leap lengths l for the trajectories resembling 'Levy flights', such as those reported in the inset. Most probable leap lengths correlate with the (001) plane spacing. Data refer to the system containing the $\Sigma 29$ (001) symmetrical twist GB.

the so-called 'Levy flights', i.e. random walks consisting of leaps arranged in a hierarchical manner [35]. As is evident from the inset of figure 9, relatively long leaps are rare but contribute to the major distance covered by the displacing atom. Long leaps then correspond to relatively long-range migrations responsible for the large rms square displacement $\langle u^2 \rangle^{1/2}$ of atoms in the less dense central region. Alternate to long leaps are segments of trajectory in which the atoms occupy approximately constant positions. A detailed analysis of the displacements undergone by 250 atoms in the GB region within a time interval of 2 ns points out that the lengths l of long leaps arrange according to the multi-modal distribution $L(l)$ shown in figure 9. The first two maxima of $L(l)$ occur at distances l correlated to the (001) plane spacing. The time intervals between long leaps are instead distributed according to a Gaussian centred at about 20 ps.

The trajectories followed by single atoms in the GB region occasionally reveal the existence of localized vortices around which groups of atoms irregularly rotate, as is also illustrated by the trajectory reported in the inset of figure 9. This occurs in particular during the course of shuffling processes involving about 20 atoms or more. The appearance of vortices can be regarded as a signature of turbulence [36]. On such a basis, the extent of atomic displacement and mixing should depend on the third power of time t [37]. However, only a roughly linear scaling of the square of the mixed layer thickness, $\delta(z_0, t)^2$, with t has been observed. This seems to be a consequence of the complex dynamics taking place within the GB region, where the trajectories of single atoms undergo continuous modifications. More specifically, for any given atom roughly involved in GB rearrangement processes, 'Levy flights' can rapidly switch into more conventional 'Brownian walks', and vice versa. Such behaviour can be related approximately to the continuous change of direction and intensity of the local mechanical forces induced by shear and this, in turn, appears to be the result of the redistribution of atomic volume within the GB region of lower density.

The atomic volume changes significantly on time scales on the order of 10 ps according to an apparently stochastic dynamics. The volume of each atom within the GB region undergoes pronounced fluctuations about an average value that is roughly equal to 1.08 v_{eq}, where v_{eq} represents the equilibrium value of the atomic volume in a relaxed bulk. As is evident from figure 10, the volume autocorrelation function, $\langle v_i(\tau)\, v_i(0) \rangle$, displays a roughly exponential time dependence. Only at very short time delays, τ, weak correlations are detectable. Such behaviour clearly indicates that volume changes are not correlated and that the redistribution

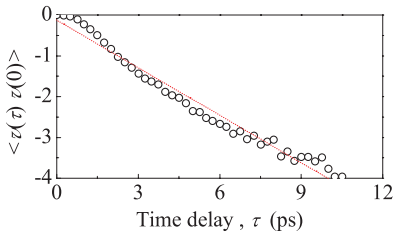

Figure 10. The semi-logarithmic plot of the autocorrelation function $\langle v_i(\tau)\, v_i(0)\rangle$ of atomic volume v as a function of the time delay τ. An exponential decrease is observed, suggesting an underlying stochastic dynamics. Weak correlations can be noted at small τ values. The best-fitted line is also shown. Data refer to atoms located within the Σ29 (001) symmetrical twist GB region.

of atomic volume within the GB region subjected to shear forces is governed by a stochastic dynamics [38].

This apparently surprising result finds support in previous work on mechano-chemical transformations under mechanical processing conditions [39].

4. Conclusions

The application of shear forces a gradual deformation of the bi-crystals containing the Σ11 (332) $\langle 110\rangle$ symmetrical tilt and the Σ29 (001) symmetrical twist GBs. The mechanical response of the systems investigated is such that the regime of elastic deformation is replaced by the regime of plastic deformation at average strain γ values of around 0.04. Above such values, the GB planes begin to slide with respect to each other. Localized shuffling processes involving the average tenths of atoms take place at the GB regions characterized by lower density. The regions at which atomic shuffling occurs represent preferential nucleation site for partial dislocations that progressively propagate into the bulk of semi-crystals. Plastic deformation at GBs is accompanied by complex dynamical processes involving the cooperative rearrangement of atomic species under the effect of shear-induced mechanical forces. Atomic displacements taking place at GBs result in the exchange of atoms between the semi-crystals separated by the rough, defected interface. The thickness of the perturbed layer involved in the mixing of atoms originally belonging to different sides of the interface shows a square-root dependence on time. Although such a power law is reminiscent of a thermal diffusion process, a different mechanistic scenario applies in the investigated cases. Atoms are indeed found to move according to highly cooperative mechanisms involving the contemporary displacement of a relatively large number of species. In addition, the dynamics of atomic shuffling processes is such that each atom keeps on average a certain number of its original nearest neighbours, even at long times. Rearrangement processes at the sheared GBs appear to be self-organized, with the atomic species undergoing alternately 'Levy flights' and 'Brownian walks', depending on the stochastic dynamics underlying the redistribution of atomic volumes under shear.

Far from being conclusive, the results discussed in the present work should be intended as a preliminary contribution to a deeper understanding of the atomic-scale processes taking place under shear. Further work is necessary to gain a detailed insight.

Acknowledgments

A Ermini of ExtraInformatica s.r.l. is gratefully acknowledged for technical support. Financial support was given by the University of Cagliari.

References

[1] Heinicke G 1984 *Tribochemistry* (Berlin: Akademie)
[2] Cahn R W and Haasen P (ed) 1996 *Physical Metallurgy* 4th revised and enhanced edn (Oxford: North-Holland)
[3] Rigney D A 2000 *Wear* **245** 1
[4] Butyagin P Yu 1989 *Sov. Sci. Rev.* B **14** 1
[5] Courtney T H 1995 *Mater. Trans. JIM* **36** 110
[6] Suryanarayana C 2001 *Prog. Mater. Sci.* **46** 1
[7] Khina B B and Froes F H 1996 *J. Met.* **48** 36
[8] Martin G 1984 *Phys. Rev.* B **30** 1424
[9] Bellon P and Averback R S 1995 *Phys. Rev. Lett.* **74** 1819
[10] Hammerberg J E *et al* 1998 *Physica* D **123** 330
[11] Fu X Y *et al* 2001 *Wear* **250** 420
[12] Lund C and Schuh C A 2003 *Appl. Phys. Lett.* **82** 2017
[13] Lund C and Schuh C A 2004 *Acta Mater.* **52** 2123
[14] Delogu F and Cocco G 2005 *Phys. Rev.* B **71** 144108
[15] Delogu F and Cocco G 2005 *Phys. Rev.* B **72** 014124
[16] Odunuga S *et al* 2005 *Phys. Rev. Lett.* **95** 045901
[17] Sansoz F and Molinari J F 2005 *Acta Mater.* **53** 1931
[18] Schonfelder B *et al* 2005 *Acta Mater.* **53** 1597
[19] Rittner J D and Seidman D N 1996 *Phys. Rev.* B **54** 6999
[20] Lutsko J F *et al* 1989 *Phys. Rev.* B **40** 2841
[21] Ducastelle F 1970 *J. Physique* **31** 1055
[22] Rosato V *et al* 1989 *Phil. Mag.* A **59** 321
[23] Cleri F and Rosato V 1993 *Phys. Rev.* B **48** 22
[24] Allen M P and Tildesley D 1987 *Computer Simulation of Liquids* (Oxford: Clarendon)
[25] Andersen H C 1980 *J. Chem. Phys.* **72** 2384
[26] Nosè S 1984 *J. Chem. Phys.* **81** 511
[27] Parrinello M and Rahman A 1981 *J. Appl. Phys.* **52** 7182
[28] Horstemeyer M F *et al* 2001 *Theor. Appl. Fract. Mech.* **37** 49
[29] Voronoi G F 1908 *J. Reine Angew. Math.* **134** 198
[30] Finney J L 1970 *Proc. R. Soc.* A **319** 495
[31] Honeycutt J D and Andersen H C 1987 *J. Phys. Chem.* **91** 4950
[32] Kelchner C L *et al* 1998 *Phys. Rev.* B **58** 11085
[33] Zhang H *et al* 2006 *Phys. Rev.* B **74** 115404
[34] Gomez L *et al* 2003 *Phys. Rev. Lett.* **90** 095701
[35] Tsallis C *et al* 1995 *Phys. Rev. Lett.* **75** 3589
[36] Solomon T H *et al* 1993 *Phys. Rev. Lett.* **71** 3975
[37] Schlesinger M F *et al* 1987 *Phys. Rev. Lett.* **58** 1100
[38] Hansen J P and McDonald I R 1991 *Theory of Simple Liquids* (New York: Academic)
[39] Foct J 2004 *J. Mater. Sci.* **39** 1